Paraffin wax removal from metal injection moulded cocrmo alloy compact by solvent debinding process

Paraffin wax removal from metal injection moulded cocrmo alloy compact by solvent debinding process

N A N Dandang[1*], W S W Harun[2], N Z Khalil[2], A H Ahmad[3], F R M Romlay[3], N A Johari [1]

[1] Institute of Postgraduate Studies, Universiti Malaysia Pahang, Lebuhraya Tun Razak, 26300 Gambang, Kuantan, Pahang, Malaysia
[2] Human Engineering Group, Faculty of Mechanical Engineering, Universiti Malaysia Pahang, 26600 Pekan, Pahang, Malaysia
[3] Manufacturing Focus group, Faculty of Mechanical and Materials Engineering, Universiti Malaysia Pahang, Pekan Pahang, 26600 Pekan, Pahang, Malaysia

*Corresponding author: nuraidahnabihahdandang@gmail.com

Abstract. One of the most crucial and time consuming phase in metal injection moulding (MIM) process is "debinding". These days, in metal injection moulding process , they had recounted that first debinding practice was depend on thermal binder degradation, which demanding more than 200 hours for complete removal of binder. Fortunately, these days world had introduced multi-stage debinding techniques to simplified the debinding time process. This research study variables for solvent debinding which are temperature and soaking time for samples made by MIM CoCrMo powder. Since wax as the key principal in the binder origination, paraffin wax will be removed together with stearic acid from the green bodies. Then, debinding process is conducted at 50, 60 and 70°C for 30-240 minutes. It is carried out in n-heptane solution. Percentage weight loss of the binder were measured. Lastly, scanning electron microscope (SEM) analysis and visual inspection were observed for the surface of brown compact. From the results, samples debound at 70°C exhibited a significant amount of binder loss; nevertheless, sample collapse, brittle surface and cracks were detected. But, at 60°C temperature and time of 4 hours proven finest results as it shows sufficient binder loss, nonappearance of surface cracks and easy to handle. Overall, binder loss is directly related to solvent debinding temperature and time.

1. Introduction

Debinding is a process that enhance the elimination of the binder component either by solvent or thermal or combination of both from the green compacts without disturbing the original form of the compact's body [1-3]. After mixing of feedstock and injection moulding, the green compact is then introduces to debinding process where the binder need to be fully removed from the feedstock [4, 5]. Besides sintering, there are one more critical phase in MIM which is call debinding [6-10]. Unsuccessful removing the maximum amount of the binder earlier can effect in compact's failings, such as cracking, collapsing and compacts will become very brittle. During sintering, inadequate removal of binder can cause infection from polymer's disintegration. Eliminating the binder without crumpling the metal particles is an elusive method and can be reached via few stages. Thermal, solvent debinding and catalytic are the most common debinding processes exist besides others method [11-13]. The aim for debinding process is to eliminate the binder's component in the possible shortest minutes besides the minimum effect on the compact. Premature debinding process is used only

thermal debinding, which mandatory more than 200 h required time to accomplishment. These days, the complete process for debinding minimised to 120 minutes depend on binder used as thermal debinding is united with solvent debinding. The benefit of solvent debinding is based on high solubility in the organic solvent of small molecular weight binder as main constituent [8, 14]. It forms networks and pore channels in the green compact thus prepare the brown compact for thermal debinding [15, 16]. When the number of pores in the compacts are huge, they lets the degraded binder which is slight constituent to simply absorb to the external of the compact's body through thermal debinding. Hence, time for thermal debinding is shorten expressively [14, 17].

Evolving a systematic considerate in process of debinding shortens debinding time and temperature. For quantity manufacture, extensive of times for debinding are impracticable for mass production. Thomas-Vielma et. al. [14] and Liu et. al. [18] exposed when solvent and thermal debinding were combine they effectively cuts time for binder removal and avoids failings after establishing in green compacts.

In this work, a paraffin wax of a low molecular weight (MW) assortment, and polypropylene (PP) and stearic acid were used as the primary, backbone binder and surfactant agent correspondingly. Among the all the binder's component, major amount of paraffin wax must be detached from a green compact in the solvent debinding process, but after debinding, PP must endure in the compact, with the purpose of holding metal particles by one and other and sustain the green compact' shape. This research concentrate on the study of solvent debinding parameters and resolve an ideal conditions for this process.

2. Experimental method

2.1. Material

Metal powder used is CoCrMo. Table 1 indicates the characteristics of metal powder. Volume of powder Loading used: 67%. Binder's components comprised of 70 vol. % paraffin wax (PW), 25 vol. % Polypropylene (PP) and 5 vol. % stearic acid (SA). The morphology of the cobalt chromium molybdenum alloy powder is shown in Figure 1. While table 1 shows the characterization results for the binders.

Table 1. Characteristics of metal powder.

Powder	Size distribution	D_{50} (μm)	D_{90}	D_{10}	S_w	Density (g/cm^3)	Shape
CoCrMo	22	11.5	23.7	4.1	3.3	8.4	Spherical

[a] Sw (slope parameter distribution = 2.56/log(D90/D10),

[b] 22 represents a particle size distribution

[c] D50 is shows the mean diameter of particle size for distribution of particle size

[c] D90 and D10 indicate the distribution at 90% and 10%,(cumulative) for size distribution curve

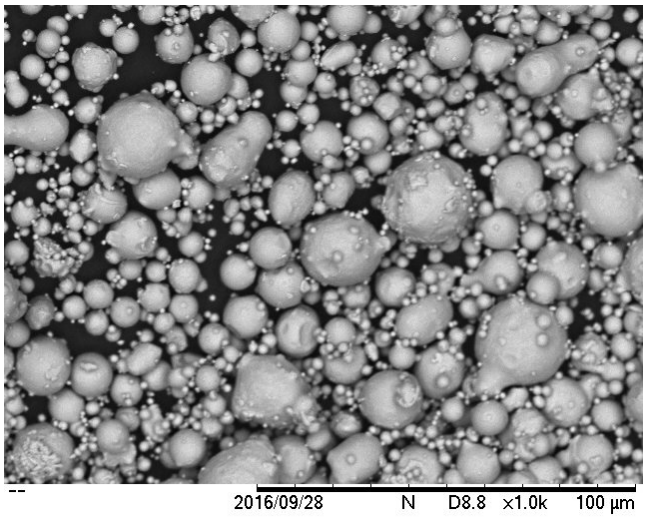

Figure 1. Morphology image of CoCrMo Alloy powder.

Table 2. A Characterization of the binders.

Binder	Chemical structure	Density (g/cm^3)	Melting temperature (˚C)	Decomposition temperature (˚C)
PW	$C_{31}H_{64}$	0.91	47-65	200-400
PP	(C3H6)n	0.90	>95	328-410
SA	$C_{18}H_{36}O_2$	0.94	69.4	180-380

2.2. Mixing of feedstock and injection moulding

Double planetary mixer at 160 °C for 90 minutes for 70 rpm rotational speed was used to prepare CoCrMo feedstock. Then, to produce a dog-bone shaped sample, injection moulding was conducted by using 200 tonne NISSEI Model NS20-2A injection moulding machine. The green compacts were successfully fabricated by injection moulding at 145 ˚ C. Based on the physical inspection, there were no defects observed on the green compacts.

2.3 Analysis of the feedstock

By using NETZSCH DSC 214 Polyma DSC21400A-01717-L machine, differential scanning calorimetry (DSC) analysis was conducted under nitrogen atmosphere on the feedstock. The start temperature for DSC test was at 0 °C until 550 °C as end temperature. Gas rate was 40ml/min and 10 °C/min was the heating rate used. While for starting and end temperatures, 10 minutes holding time was used throughout this process.

2.4 Solvent debinding

Figure 2 shows schematic diagram of solvent debinding process by wicking technique. Here, samples been placed in a condenser after been compacted. Then, the samples were debound at 50, 60 until 70 ˚C temperatures. The debinding times were 30 to 240 minutes (4 hours). From Figure 3, the illustrations of graph for solvent debinding process been utilised. About 40 ml n-heptane was used as a solvent in this debinding process by wicking technique using Al_2O_3 powders. This powder bed helps to avoid distortion and it offers more uniform heating through this process [1]. Then, as the brown compacts were obtained from this process, the amount of weight loss for each compacts for each conditions as stated will be measured.

From equation 1 below, Mpw indicates the mass loss of paraffin wax where the mass of PW and SA were been calculated based on the equation below:

$$Mpw\ (\%) = \frac{Mb-M}{Mb} x\ 100 \quad (1)$$

Where Mb is the mass before solvent debinding (green compact) and Ma is the mass after solvent debinding of the (brown compact)

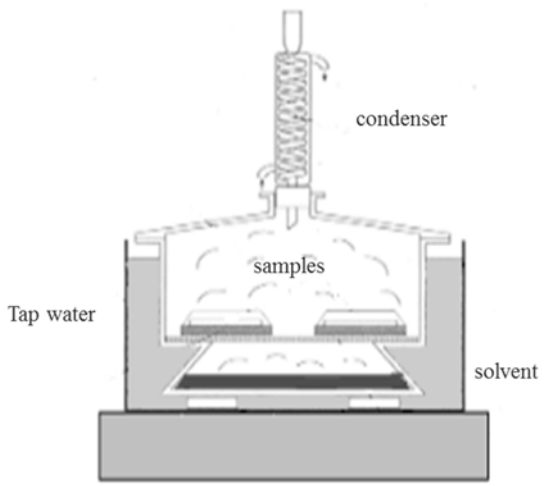

Figure 2. Schematic diagram for solvent debinding by wicking technique.

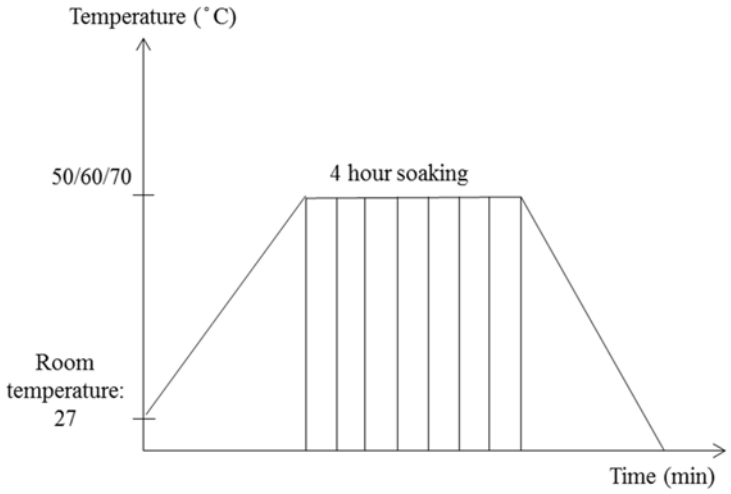

Figure 3. Graph illustrates Time vs Temperature plot of solvent debinding.

3. Results and discussion

Feedstock was successfully moulded using a Nissei NS20-2A injection moulding machine and debound by wicking technique. Defect free green and brown compacts are produced as shown in Figure 4.

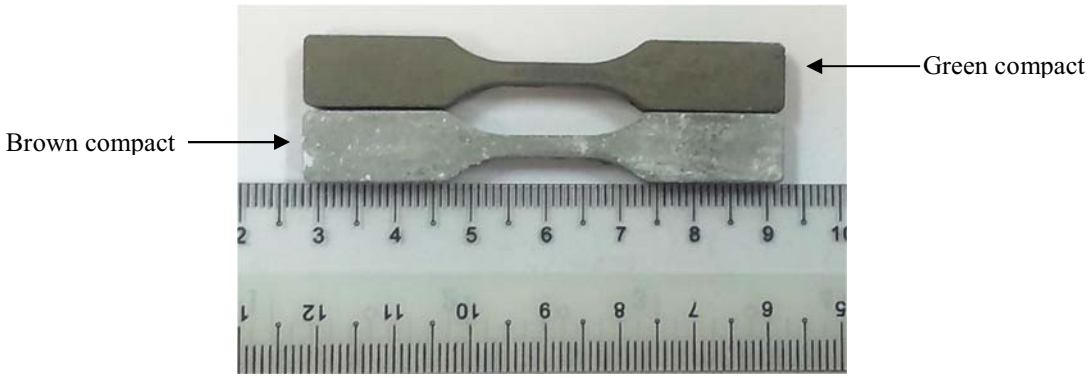

Figure 4. Green and brown compact of CoCrMo Alloy without defects.

3.1. DSC of the feedstock

The injection moulding and solvent debinding temperatures were predicted by thermal properties of feedstock as it offers an excellent guide for future experiment in this research. From Figure 5, it can be observed 57.5 – 167.5 ˚C is the uttermost feedstock's melting temperatures. As shown in the Figure, first peak of the curve shows the melting point of paraffin wax and stearic acid. While, for polypropylene, the highest peak, which is the second peak specified the melting of polypropylene. From Hwang et. al. [12] it was stated that, when the melting point of the maximum melting binder component is surpassed, the binder becomes more flowable.

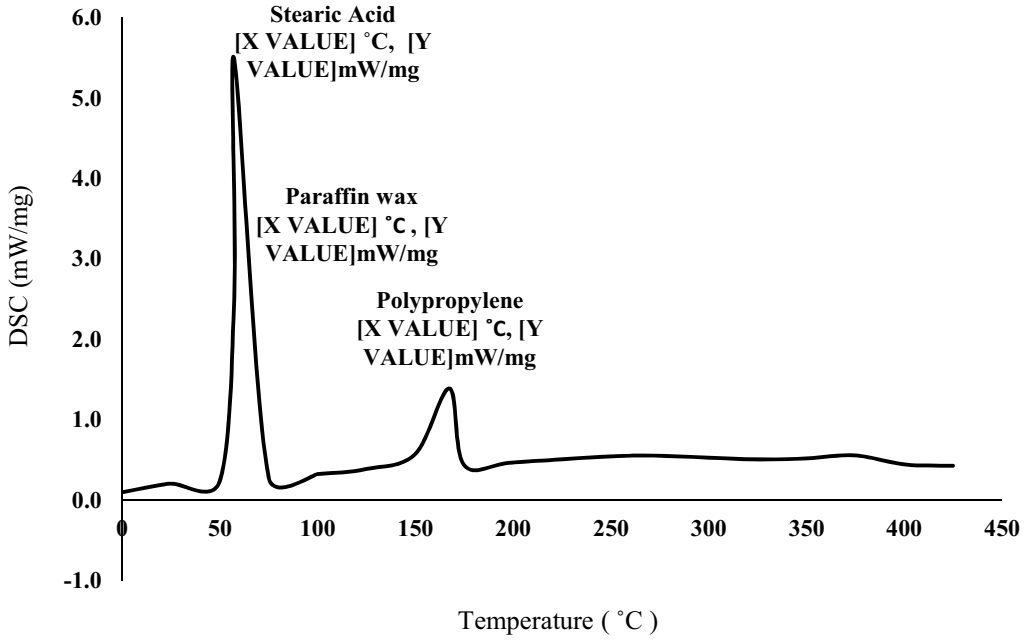

Figure 5. Feedstock's DSC analysis.

3.2. Solvent debinding

To reduce time for debinding, thermal debinding and solvent debinding techniques had been introduced. Then, the parameters for this process were enhanced using results from DSC test. The function of solvent solution used, which is n-heptane was to remove paraffin wax and stearic acid. Then, a porous brown compact was formed once they had been removed. The existence of pores in the

compacts enables backbone binder which is polypropylene (PP) to diffuse out during thermal debinding process.

Figure 6 shows the mass loss of paraffin wax at numerous temperatures. In the first hour of process, it can be presumed that as the debinding temperature increase, the loss of the binder also increase. Hence, when temperatures increase, it boost binder diffusivity and solubility. Besides, more binder loss with the extended of debinding time. Correspondingly, it can be illustrated from Figure 7 that 4 phases occur throughout solvent debinding. Based on Md Ani et. al. work [19], the phases of process are discussed.

Phase I [0-60 minutes]: During this phase, loss of binder's component were quite fast as they are directy contact with the solvent on the surface.

Phase II [60-120 minutes]: The rate of debinding decelerates. It is due to the solvent that enter intensely into the compact and the binder was extracted and liquefy into the surface. Capillary forces helped the dissolved binder to diffuse to the exterior surface of compact by liquid extraction [3, 20].

Phase III [120-180 minutes]: The debinding rates start to rise due to an adequate channels formed in the compact that permits the dispersion of the binder dissolved rapidly to the exterior surface of compact. From the graph, the incline is the highest at 70 ˚C which can be proved that the debinding rate achieves it peaks at this phase. At 50 °C and 60 °C temperatures, debinding rates on graph seem to be going at the similar leap. While, on curve 70 °C, the debinding rate is reasonably high.

Phase IV [180-240 minutes]: From the graph, the mass loss of binder remains constant when temperature increase and cause the debinding rate reduces. From this phase, the saturation point of solvent and the binder had been achieved. But, it should be alert that the stability point among the latter is reliant on the solvent-binder component volume ratios.

The compassion of binder diffusivity and solubility to changes of temperature can be seen from the graph of debinding rate at 50 and 60˚C. For phases II-IV which is at 50°C, the debinding rate seems to be consistently reduces, where inclines are nearly constant. In contrast, at 60 °C, phases II – IV, the debinding rate seems to increase until 180 minutes. Figure 8 illustrates the overview of solvent debinding mechanism, besides the conditions of the binder and diffusion of solvent during debinding. Debinding rates throughout debinding process are reliant on movement of molecules from dissolved binder, where they commonly move more rapidly with increasing of temperatures and smaller solvent molecules as reported by German and Bose.

Researchers had stated that, when the temperature of solvent debinding exceeds highest melting point of the soluble binder components, MIM compacts will start to collapse. Figure 9 shows compacts are collapse and cracks after solvent debinding. High solvent temperatures, longer debinding times, and thickness variation of the component are the reasons behind all those conditions from the Figure 9. The compact will crack due to insoluble binder component due to longer soaking time. Besides, higher temperature makes binder soften which effects green compact to crack. Therefore, it is why cracking demonstrates on the surface of compact as shown in Figure 9. These external defects were detected from the compact debound at 70 °C for 240 minutes debinding time. Compact debound at 60 °C temperature shows efficient amount of paraffin wax mass loss after 240 minutes with no defects on the surface existing on the compact.

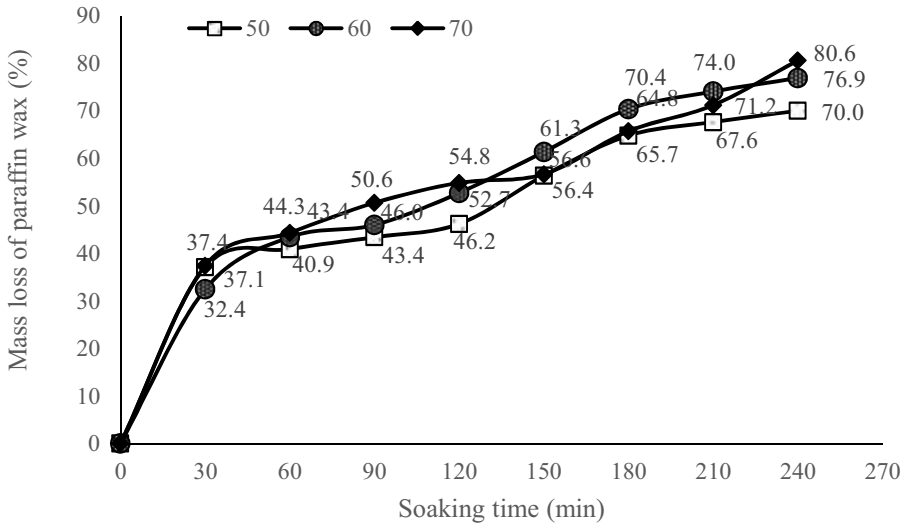

Figure 6. Time vs Temperature plot for paraffin wax's mass loss during solvent debinding.

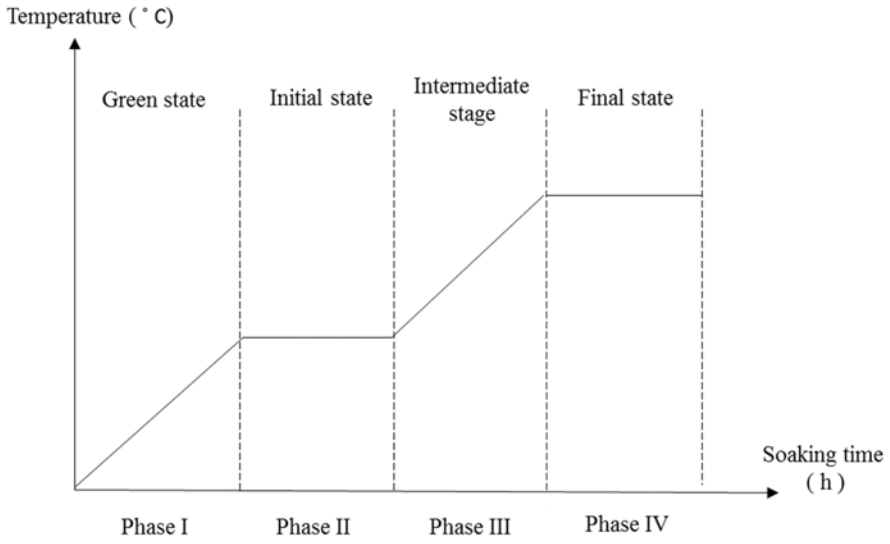

Figure 7. A schematic graph of paraffin wax loss for each phases.

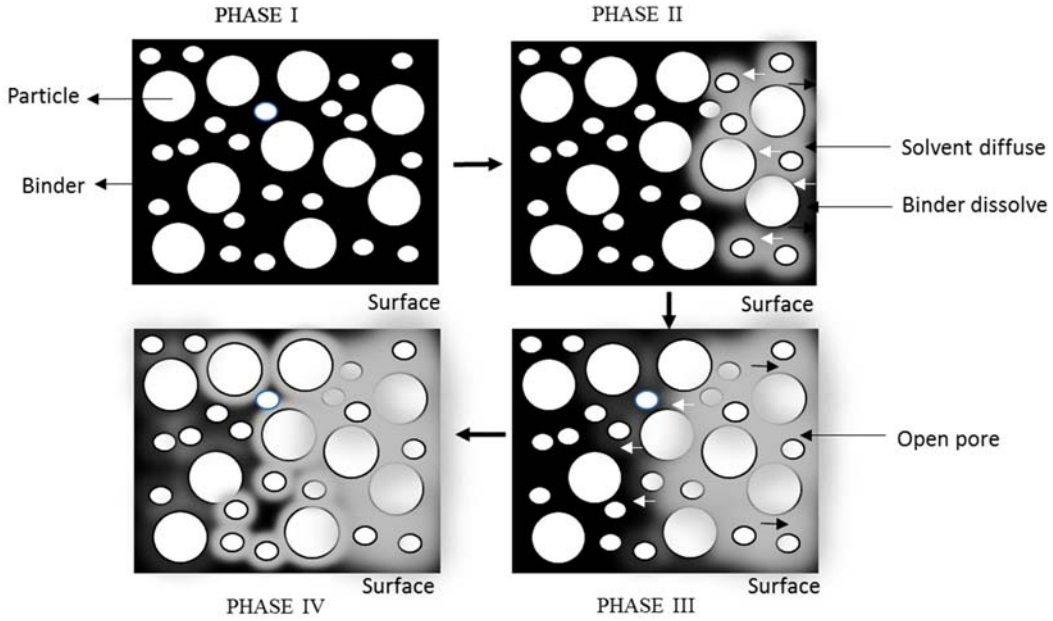

Figure 8. A schematic Figure presenting the interaction between solvent and binder diffusion occur during wicking debinding process.

(a)

(b)

(c)

Figure 9. Defects observed on brown compact a) Fractures b) collapse c) cracks at conditions 70 ˚C and 4 hour.

From Figure 10, SEM micrographs demonstrate the microstructure image of compacts before and after solvent debinding. From the Figure, it can be realised that the metal particles was squarely scattered in the binder matrix. Then, uniform binders distribution can also been detected in the compact. After solvent debinding, it is clear that, open pore channels had formed besides PW and SA binders had been removed but there are still remaining binder to retain the shape of the compact before thermal debinding which is PP.

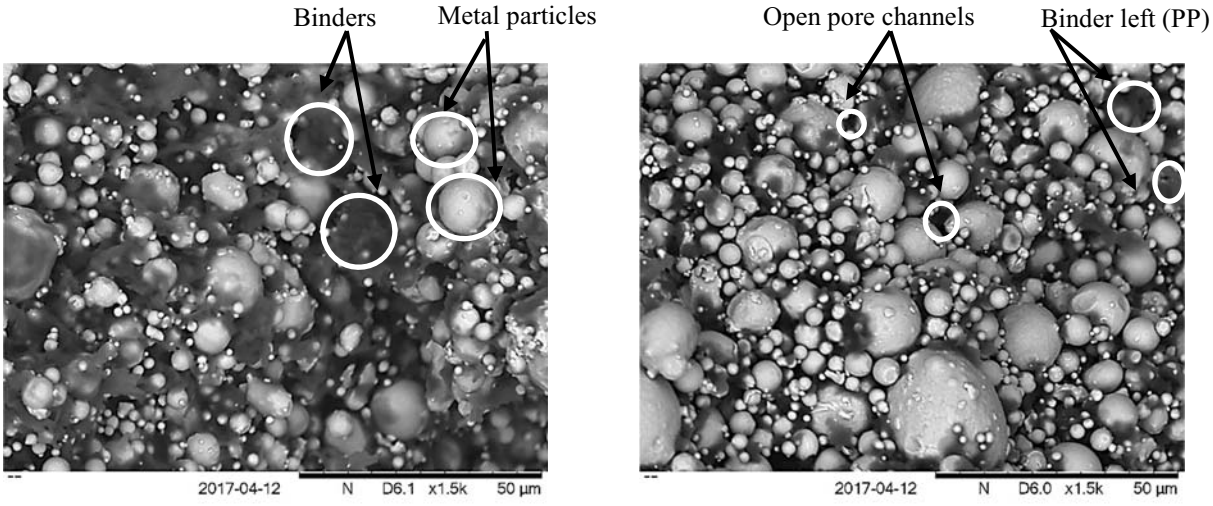

Figure 10. SEM micrographs of green compact before solvent debinding (a) and brown compact after solvent debinding (b).

4. Conclusions

From the above research work, we can conclude following:

- Based on DSC graph result from Figure 5, it was proven that the melting point of each binder's component which is Paraffin Wax (PW), Polypropylene (PP) and Stearic Acid (SA) had been achieved. Therefore, it makes them becomes more flowable and appropriate to be used as selected binder component in this research study.
- To achieve an ideal conditions of solvent debinding, the process had been completed at different parameters. From the results, debinding temperatures and soaking time significantly influences the mass loss of paraffin wax of compacts. The significant amount of mass loss of paraffin wax whics 76.9% without no defects on the brown compacts shows an ideal condition for solvent debinding of CoCrMo alloy compact.
- The ideal and an optimum condition of solvent debinding for CoCrMo alloy is suitable at the condition of 60 °C for 4 hours, using n-heptane solution with 40 ml volume.
- This can be proved from SEM image results from Figure 10, where at conditions 60℃ and 4 hours soaking time, Paraffin Wax had been removed and open pore channels are formed which shows that, the binder is successfully been removed at this condition.

Acknowledgements

Universiti Malaysia Pahang fully supports the facilities and resources for this research. The author W.S. W. Harun would like to acknowledge the support of the internal grant of Universiti Malaysia Pahang RDU141101, RDU140354, RDU150337 and the support of Research Acculturation Collaborative Effort (RACE) provided by the Ministry of Higher Education, Malaysia RDU151314.

References

[1] German R M and Bose A 1997 *Injection molding of metals and ceramics*: Metal Powder Industries Federation)
[2] German R M, Bose A and Mani S S 1992 Sintering time and atmosphere influences on the microstructure and mechanical properties of tungsten heavy alloys *Metallurgical Transactions A* **23** 211-9
[3] BECKER F H 2006 Debinding processes: Physical and chemical conclusions and their practical realisations. In: *CFI. Ceramic forum international*: Göller)

[4] Ye H, Liu X Y and Hong H 2008 Sintering of 17-4PH stainless steel feedstock for metal injection molding *Materials Letters* **62** 3334-6
[5] Onbattuvelli V P, Chinn R, Enneti R K, Park S-J and Atre S V 2014 The effects of nanoparticle addition on binder removal from injection molded silicon carbide *Ceramics International* **40** 13861-8
[6] Zhu B, Qu X and Tao Y 2003 Mathematical model for condensed-solvent debinding process of PIM *Journal of materials processing technology* **142** 487-92
[7] OMAR M, SAUTI R and ABDULLAH N DEBINDING AND SINTERING CHARACTERISTIC OF INJECTION MOULDING CoCrMo ALLOY POWDER FOR BIOMEDICAL APPLICATIONS
[8] Yang W-W, Yang K-Y, Wang M-C and Hon M-H 2003 Solvent debinding mechanism for alumina injection molded compacts with water-soluble binders *Ceramics International* **29** 745-56
[9] Chen G, Cao P, Wen G and Edmonds N 2013 Debinding behaviour of a water soluble PEG/PMMA binder for Ti metal injection moulding *Materials Chemistry and Physics* **139** 557-65
[10] Wongpanit P, Khanthsri S, Puengboonsri S and Manonukul A 2014 Effects of acrylic acid-grafted HDPE in HDPE-based binder on properties after injection and debinding in metal injection molding *Materials Chemistry and Physics* **147** 238-46
[11] Sidambe A T, Figueroa I A, Hamilton H G C and Todd I 2012 Metal injection moulding of CP-Ti components for biomedical applications *Journal of Materials Processing Technology* **212** 1591-7
[12] Hwang K, Lin H and Lee S 1997 Thermal, solvent, and vacuum debinding mechanisms of PIM compacts *Material and Manufacturing Process* **12** 593-608
[13] Hayat M D, Wen G, Zulkifli M F and Cao P 2015 Effect of PEG molecular weight on rheological properties of Ti-MIM feedstocks and water debinding behaviour *Powder Technology* **270, Part A** 296-301
[14] Thomas-Vielma P, Cervera A, Levenfeld B and Várez A 2008 Production of alumina parts by powder injection molding with a binder system based on high density polyethylene *Journal of the European Ceramic Society* **28** 763-71
[15] Li B Q, Wang C Y and Lu X 2013 Effect of pore structure on the compressive property of porous Ti produced by powder metallurgy technique *Materials & Design* **50** 613-9
[16] Páez-Pavón A, Jiménez-Morales A, Santos T G, Quintino L and Torralba J M 2016 Influence of thermal debinding on the final properties of Fe–Si soft magnetic alloys for metal injection molding (MIM) *Journal of Magnetism and Magnetic Materials* **416** 342-7
[17] Zaky M 2004 Effect of solvent debinding variables on the shape maintenance of green molded bodies *Journal of materials science* **39** 3397-402
[18] Liu Z, Loh N, Tor S, Khor K, Murakoshi Y and Maeda R 2001 Binder system for micropowder injection molding *Materials Letters* **48** 31-8
[19] Md Ani S, Muchtar A, Muhamad N and Ghani J A 2014 Binder removal via a two-stage debinding process for ceramic injection molding parts *Ceramics International* **40** 2819-24
[20] Chikwanda H and Machaka R 2014 A study of solvent debinding variables on Ti6Al4V green bodies